Int. J. Electrochem. Sci., 13 **(2018)** 6734 – 6755, doi: 10.20964/2018.07.23

International Journal of ELECTROCHEMICAL SCIENCE
www.electrochemsci.org

Inhibitive Properties and Quantum Chemical Calculations of a New Synthesized Schiff Base 1-[(3hydroxyphenylamino) methylene]-naphtalen-2-one for XC48 in Hydrochloric Acid Solution

Bouzidi Leila[1,*], *Haffar Djahida*[1], *Abdi Djamila*[2], *Mouzali Saida*[1], *and Chafaa Salah*[1]

[1] Laboratory of Electrochemistry of Molecular Materials and Complexes (LEMMC), Department of Engineering Process, Faculty of Technology, University of Setif 1, Algeria
[2] Laboratoire d'énergétique et d'électrochimie du solide, Department of Engineering Process, Faculty of Technology, University of Setif 1, Algeria
[*]E-mail: leila.8207@yahoo.fr

Received: 16 January 2018 / *Accepted:* 2 April 2018 / *Published:* 5 June 2018

A new Schiff base derived from o-hydroxy aromatic aldehyde, namely 1-[(3-hydroxyphenylamino) methylene]-naphtalen-2-one (L), was synthesized and characterized by X-ray crystallographic technique. It is then evaluated as inhibitor on the corrosion of mild steel XC48 in a 1M hydrochloric acid solution. The study was carried out using weight loss, polarization, electrochemical impedance spectroscopy and Quantum chemical. At constant temperature, the corrosion rate decreases with increasing the inhibitor content. A maximum inhibition efficiency of 78.3 % was obtained at 10^{-3} M. However, the increase in temperature leads to an increase in the corrosion rate of steel. Calculation and estimation of thermodynamic parameters E_a, $\Delta H°_{ads}$, $\Delta S°_{ads}$, and $\Delta G°_{ads}$ help in determining the inhibition mechanism of the Schiff base. It was found that Schiff base acted as mixed type inhibitor with predominant cathodic inhibition and adsorbs according to Langmuir adsorption isotherm model. Morphological surface aspect has been investigated using optical microscope. Quantum chemical calculations study corroborates experimental results.

Keywords: Synthesis; Mild steel; Weight loss; Adsorption; Polarization; Impedance

1. INTRODUCTION

Corrosion of mild steel is largely studied in the last decade because of the severe encountered degradation problems which steems from the industrial use of this later in aqueous acidic solution namely sulphuric acid and hydrochloric acid. To remedy such problem the use of inhibitors remains the most practical method for protection against corrosion in acidic media [1, 2]. These later acts only

when added to the medium in small quantities. They can control, minimize, or prevent direct reactions between a metal and its environment.

Several organic compounds, such as triazole derivatives [3], Schiff bases [4-6], macrocyclic polyether compounds [7] have been investigated as corrosion inhibitors. The Schiff bases are organic ligands which contain azomethine group (R-C=N-). They are generally prepared by condensation of primary amines ($-NH_2$) with carbonyl compounds (aldehydes or ketones).

Schiff bases have been tested for various steels in acid media [5, 6,8]. Certain Schiff bases compounds have demonstrated their effectiveness as corrosion inhibitors, not only to mild steel but also aluminum, copper and zinc in an acid medium [9-13]. These substances generally become effective by adsorption on a metal surface.

Many attempts to reduce metals attacks have been done by using organic compounds, particularly those containing heteroatoms like nitrogen, phosphorus, oxygen, sulfur, as well as aromatic rings and due to the free electron pairs they possess [8, 14]. These heteroatoms play a leading role in this interaction by donating their free electron pairs [15, 16].

In addition, compounds with multiple bonds behave as efficient inhibitors due to the availability of π-electrons for interaction with the metal surface.

In this study, we report first the synthesis of a new Schiff base derived from o-hydroxy aromatic aldehyde 1-[(3-hydroxyphenylamino)methylene]-naphtalen-2-one (L) with its structural analysis carried out using X-ray crystallographic technique.

The inhibiting action of this newly synthesized ligand derived from m-aminophenol and 2-hydroxy naphtalaldehyde, towards the corrosion behavior of steel in 1 M hydrochloric acid (HCl) solution has been studied using weight loss, polarization, electrochemical impedance spectroscopy (EIS) techniques. Theoretical studies and quantum calculations using chemical reactivity descriptors such as energy of highest occupied molecular orbital (E_{HOMO}), energy of lowest unoccupied molecular orbital (E_{LUMO}), energy gap (ΔE), dipole moment (μ), electronegativity (χ), global hardness (η), softness (σ), the fraction of electrons transferred (ΔN) have been employed to complete the experimental results. It is also the purpose of this work to investigate the adsorption characteristics and inhibition performance of this compound and the effect of temperature on mild steel corrosion in 1M HCl solution.

2. EXPERIMENTAL

2.1. Preparation and characterization of new Schiff base 1-[(3-hydroxyphenylamino)methylene]-naphtalen-2-one (L)

The reagents used for the synthesis are 2-hydroxynaphthaldehyde and m-aminophenol (Merck), without purification. The compound 1-[(3-hydroxyphenylamino)methylene]-naphtalen-2-one (L) was prepared as described in the literature [17-19]. A mixture of 2-hydroxynaphtalaldehyde (1 mmol) in absolute ethanol (10 ml) and m-aminophenol (1 mmol) in absolute ethanol (10 ml) was refluxed with boiling for 3 hours under constant stirring.

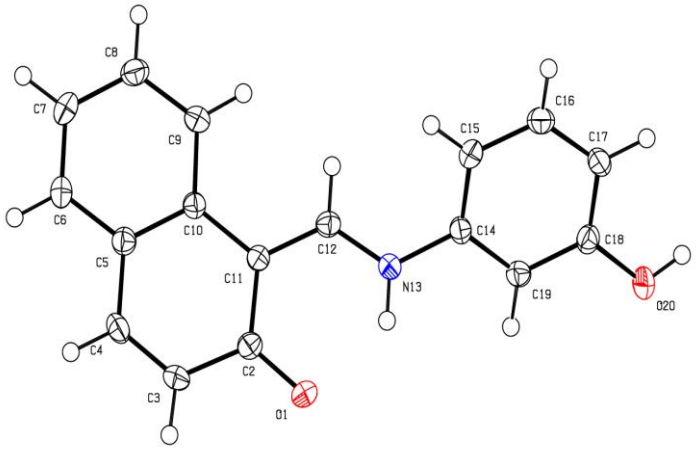

Figure 1. The molecular structure of 1-[(3-hydroxyphenylamino)methylene]-naphtalen-2-one (L)

Table 1. Crystal data and structure refinement for compound 1-[(3-hydroxyphenylamino) methylene]-naphtalen2-one (L).

Empirical formula	$C_{17}H_{13}NO_2$
Formula weight	263.28
Temperature	150(2) K
Wavelength	0.71073 Å
Crystal system, space group	Orthorhombic, P c a b
Unit cell dimensions	a = 6.8267(4) Å alpha = 90 deg. b = 15.0824(10) Å beta = 90 deg. c = 24.2466(17) Å gamma = 90 deg.
Volume	2496.5(3) $Å^3$
Z, Calculated density	8, 1.401 Mg/m^3
Absorption coefficient	0.092 mm^{-1}
F(000)	1104
Crystal size	0.22 x 0.22 x 0.12 mm
Theta range for data collection	3.18 to 27.47 deg.
Limiting indices	-8<=h<=8, -17<=k<=19, -31<=l<=27
Reflections collected / unique	16894 / 2853 [R(int) = 0.0582]
Completeness to theta = 27.47	99.8 %
Absorption correction	Semi-empirical from equivalents
Max. and min. transmission	0.989 and 0.875
Refinement method	Full-matrix least-squares on F^2
Data / restraints / parameters	2853 / 0 / 182
Goodness-of-fit on F^2	1.010
Final R indices [I>2sigma(I)]	R1 = 0.0466, wR2 = 0.1032
R indices (all data)	R1 = 0.0819, wR2 = 0.1240
Largest diff. peak and hole	0.192 and -0.264 e. $Å^{-3}$

The color of the reacting mixture changed to yellow. The precipitate was collected and washed with a small amount of cold ethanol (yield 90 %, m.p 250 K). Crystal of compound 1-[(3-hydroxyphenylamino)methylene]-naphtalen-2-one (L) was obtained by slow evaporation of an ethanol solution. The ligand L product was identified by X-ray diffraction (XRD).

The asymmetric unit is shown in Fig. 1; we confirm the empirical formula of the title compound which is $C_{17}H_{13}NO_2$, with molar mass 263.28.This compound crystallizes in the orthorhombic space group P c a b with the following dimensions of unit cell a shown in table 1: a = 6.8267(4), b = 15.0824(10), c = 24.2466(17), V = 2496.5 (3) $Å^3$, density d = 1.401 $g.cm^{-3}$. The crystal structure was solved by Refinement method full-matrix least-squares on F^2. Final R indices [I > 2 sigma (I)] (R1 = 0.0466 and wR2 = 0.1032), R indices (all data) (R1 = 0.0819 and wR2 = 0.1240) for 16894 reflections.

Crystal data and structure refinements for compound L are reported in Table 1. Selected bond lengths are given in Table 2. Crystallographic data for the structure of compound L has been deposited in the Cambridge Crystallographic Data Centre (deposition number CCDC 983634).

Table 2. Some selected Bond lengths (Å) for compound 1-[(3-hydroxyphenylamino) methylene]-naphtalen2-one (L)

Bond	lengths (Å)	Bond	lengths (Å)
C(2)-O(1)	1.275(2)	C(2)-C(11)	1.445(2)
C(2)-C(3)	1.447(2)	C(3)-C(4)	1.346(2)
C(10)-C(11)	1.461(2)	C(11)-C(12)	1.395(2)
C(12)-N(13)	1.324(2)	N(13)-C(14)	1.427(2)
N(13)-H(13)	0.8800	C(14)-C(15)	1.387(2)
C(14)-C(19)	1.392(2)	C(18)-O(20)	1.364(2)
C-H	0.9500	O(20)-H(20)	0.840

The positions of the hydrogen atoms bonded to carbon atoms were calculated (C-H distance 0.95 Å).

Thus, the O1–C2 bond distance of 1.275 (2) Å is also consistent with the C=O double bonding.

A similar effect was observed for N-n-propyl-2-oxo-1-naphthylidene methylamine [C=O 1.277 (2) Å] [20] and 1-[(3-hydroxypyridin-2-ylamino) methylene]- 1H-naphthalen-2-one [C=O 1.276 (2) Å] [21]. The C=O bond distance 1.275 (2) Å indicates the presence of the keto form, with a partial double bond character of the CO group. In the compound, the C=O bond lengths vary from 1.261 (4) to 1.307 (5) Å due to tautomerism influence. These values are in good agreement with our study.

This property is caused by proton transfer from the hydroxyl O atom to the imine N atom (N13—H13 distance 0.88 Å).

The short C2—O1 = 1.275 (2) Å and C11—C12 = 1.395 (2) Å bonds can be considered as C=O and C=C double bonds, respectively.

The Structure of compound L reveals that the keto tautomer is favored over the enol tautomer. This is evident from the observed O1–C2 bond distance of 1.275 (2) Å, which is consistent with the O–C double bond; similarly the N13–C12 distance of 1.324 (2) Å is also consistent with the N–C single bonding [18].

From the X-ray diffraction experiment, the presence of keto-amine tautomer was proved.

2.2. Chemicals and electrodes

Hydrochloric acid (Merck 36%) was used as corrosive media and prepared by dilution with bidistilled water to obtain (1M HCl). The concentration range of inhibitor used was from 10^{-5} to 10^{-3}M in 1 M HCl.

The mild steel XC48 used as working electrode present the following chemical composition: C 0.52-0.50 %, Mn 0.5-0.80 %, Si 0.40 %, P 0.035 %, S ≤ 0.035 % and remainder iron.

The surface of specimens was polished successively by graded metallographic emery papers (800 and 2000 grad) until the obtention of clean surface free from apparent defects, then degreased with acetone, washed with bidistilled water and finally dried at room temperature.

2.3. Weight loss measurements

Cylindrical steel Specimens of size (diameter 1 cm, length 0.9 cm) were immersed in different concentrations of inhibitor solutions taken in glass bottles in inclined position.

Before and after the immersion the mass of mild steel samples was weighed using analytical balance 0.0001 g accuracy and before immersion the steel specimens were polished successively with different grades emery paper (400, 600, 800, 1200 and 2000), washed with bidistilled water and cleaned with acetone.

Equations 1 and 2 were used to calculate weight loss measurements (w), inhibition efficiency (%), corrosion rate (C_R) and surface coverage (Θ) for various inhibitor concentrations as follows [22].

$$\theta = \frac{w_o - w_i}{w_o} \quad (1)$$

Where, w_0 and w_i are the weight loss values in presence and absence of inhibitor, respectively.

$$C_R = \frac{87.6\, w}{a\, t\, D} \quad (2)$$

Where, w is corrosion weight loss of mild steel (mg), a is the area of the coupon (cm^2), t is the exposure time (h) and D the density of mild steel ($mg.cm^{-3}$).

2.4. Electrochemical measurements

A PGZ 301 Voltalab 40 model potentiostat/galvanostat connected with Pentium IV computer has been used for electrochemical measurements at temperature room.

In our experiments, all electrochemical studies were performed in a conventional three electrode thermostated cell with double wall (Tacussel Standard CEC/TH). The working electrode was inserted in Teflon tube and isolated with polyester so that only its section was allowed to contact the aggressive solutions. The reference electrode is a standard calomel electrode (SCE) and the counter electrode (CE) is a graphite carbon rod.

Potentiodynamic polarization curves were carried out in the potential range from 0 to - 600 mV relative to the open circuit potential with a scan rate of 0.5 mV/s. Electrochemical tests were realized at room temperature. Each experiment has been repeated three times under the same conditions. Prior to each measurement, the electrode surface was pretreated by the same manner as for weight loss experiments. All experiments were performed out in aerated unstirred solutions.

Electrochemical impedance spectroscopy (EIS) measurements were carried out at room temperature after a stationary state was achieved within a frequency range between 100 kHz and 10 mHz with a decreasing scanning frequency order and an ac amplitude of 10 mV. Before each experiment the surface of the electrode was prepared similarly as previously described.

Each impedance spectrum was simulated with the software "Z_{ViewII}" and the best fitting was achieved by applying an electric circuit model. To obtain the stabilized open circuit potential (OCP), the samples were immersed for 30 min in the solution before EIS and Tafel polarization measurements.

2.5. Surface morphology

Mild steel surface morphology was analyzed by optical microscope using Olympus Optical model TH4-200. The investigated samples were recorded after 24, 48 and 96 hrs exposure time in test solutions in the absence and the presence of our inhibitor L.

2.6. Quantum chemical calculation

Quantum chemical calculation using density functional theory (DFT) was performed to explore the relationship between the molecular properties of the inhibitors and their subsequent inhibition efficiencies.

The molecular optimization was carried out using the density function theory (DFT)/B3LYP with basis set 6-31G. Theoretical parameters such as the highest occupied molecular orbital (E_{HOMO}), lowest unoccupied molecular orbital (E_{LUMO}) energy levels, energy gap ($E_{LUMO} - E_{HOMO}$), dipole moment (μ), global hardness (η), softness (σ), and the fraction of electrons transferred from the inhibitor molecule to the metal surface (ΔN) were calculated and discussed.

3. RESULTS AND DISCUSSION

Weight loss, linear polarization, electrochemical impedance spectroscopy methods are techniques which complement each other; they were used systematically in order to monitoring the

inhibitive properties of compound L on the corrosion process. The surface morphology of the mild steel samples was investigated after the corrosion attack products were removed from the surface.

3.1. Weight loss measurements

3.1.1. Effect of inhibitor concentration

In Table 3 are gathered weight loss measurements values of the inhibition efficiency and corrosion rate of mild steel with different concentrations of inhibitor L in acid media (1 M HCl) at room temperature after 6 h of immersion.

It can be seen that the inhibition efficiency increases with enhancement of the concentration inhibitor, and the optimum concentration of best inhibitor efficiency is obtained with 10^{-3} M (η % = 78.3 %). The inhibition process of mild steel by ligand L can be explained in terms of adsorption on the metal surface.

In fact metal surface adsorption of inhibitor L occurs thanks to the interaction between the pairs of oxygen electrons and the unsaturation of this later and the metal surface. The presence of vacant orbitals of low energy in iron atom facilitated this process; such behavior is observed in the transition group metals. The studied compound acts by getting adsorbed on the mild steel surface blocking the active sites and reducing both of the anodic and the cathodic reactions.

Table 3. Corrosion parameters and free energy adsorption obtained from weight loss measurements for mild steel in 1 M HCl in presence of different concentrations of compound 1-[(3-hydroxyphenylamino) methylene]-naphtalen2-one (L) at 292 K for 6h.

Inhibitor (M)	Weight loss (mg)	C_R (mm $year^{-1}$)	η_{WL} (%)	Θ	k_{ads} ($x10^4 M^{-1}$)	ΔG_{ads} (KJ mol^{-1})
1M HCl	1.36	0.43	……	……..	…….	……..
$1\cdot10^{-5}$	1.09	0.34	19.60	0.19	2.40	-34.22
$5\cdot10^{-5}$	0.77	0.24	43.50	0.43	1.50	-33.08
$1\cdot10^{-4}$	0.65	0.20	52.17	0.52	1.09	-32.30
$5\cdot10^{-4}$	0.50	0.15	63.00	0.63	0.34	-29.47
$1\cdot10^{-3}$	0.30	0.09	78.30	0.78	0.36	-29.61

3.1.2. Adsorption isotherm and thermodynamic parameters results

As mentioned before, the adsorption process of organic inhibitor onto the metal is affected by the chemical structure of organic molecules, the nature of metal, its charge, and the type of aggressive media [23, 24].

Four types of adsorption at the metal/solution interface by organic molecules are reported in the theory: (a) Electrostatic attraction between charged metal and molecules; (b) Interaction of molecule

uncharged electron pairs with the metal; (c) Interaction of π electrons with the metal, and (d) combination of step (a) with step (c).

In chemisorption process we have formation of coordinate type bond involved by the charge transfer from the molecules to the metallic surface ; this could be favored by the existence of the d vacant low-energy orbitals in the metal surface [25].

The study of adsorption isotherm provides us interesting information on the interaction between the inhibitor and the metal surface and helps to understand better the mechanism of adsorption.

As shown in Fig. 2, suitable adsorption isotherm were obtained using weight loss measurements and the relation (3).

$$\frac{c_{inh}}{\theta} = \frac{1}{K_{ads}} + c_{inh} \qquad (3)$$

In fact the linear relationship (3) of $\frac{c_{inh}}{\theta}$ versus c_{inh} drawn in Fig. 2, demonstrates that ligand L adsorption on the mild steel obeyed the Langmuir adsorption isotherm (which fits best to the surface coverage).

This isotherm is represented with high correlation coefficient (R^2 = 0.99) and it assumes that the adsorption of organic molecule on the adsorbent is monolayer.

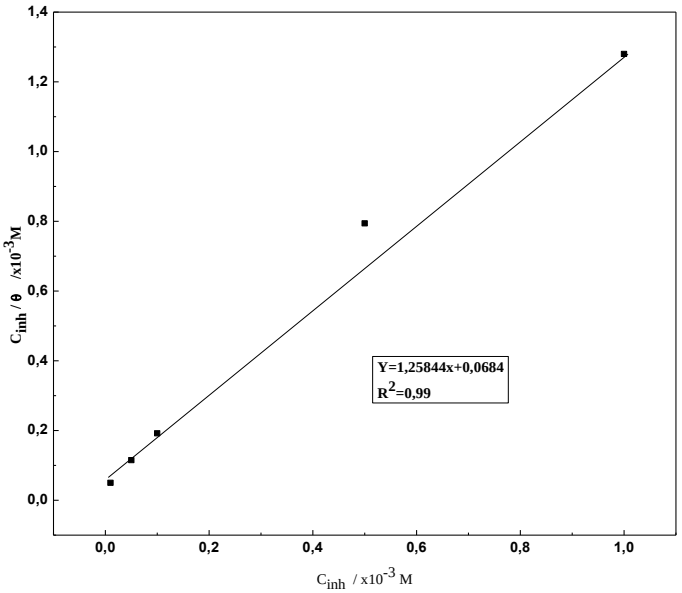

Figure 2. Langmuir adsorption of compound L on the mild steel surface in 1 M HCl solution.

The exploitation of Langmuir adsorption isotherm permits the estimation of an important factor which is the equilibrium constant (K_{ads}) value, for ligand L 1.45×10^4 M^{-1}. This later lead to adsorption standard free energy according to equation (4):

$\Delta G°_{ads} = -RT \ln (55.5\ K_{ads})$ (4)

The calculated $-\Delta G°_{ads}$ values included in Table 3 are ranging between 29 and 34 kJ/mole. One can remark that spontaneous adsorption process is confirmed by the negative signe of $\Delta G°_{ads}$ and the range values show that both physical and chemical adsorptions took place as observed by Al-Moubaraki [26].

3.1.3. Effect of temperature

Corrosion process is generally activated by temperature among other factors, for this reason we have studied its influence on the inhibition efficiencies of ligand L. Weight loss measurements were performed in the temperature range 292 - 330 K in the absence and presence of 10^{-3} M inhibitor L.

Corrosion parameters resulted from this study are gathered in Table 4. It is obvious that the increase in temperature leads to the enhancement of the corrosion rate of steel in both cases in absence or in presence of inhibitor L.

At constant concentration of inhibitor L, the η_{wl} decreases with increasing temperature and show the C_R increases. This can be attributed to the partial desorption of the inhibitor L from the metal surface under temperature effect causing increase in the dissolution process.

Arrhenius equation is introduced in order to show the dependence of the corrosion rate with temperature:

$$C_R = \lambda \exp\left(-\frac{E_a}{RT}\right) \quad (5)$$

Where E_a is apparent activation energy for the corrosion of mild steel in HCl solution, R the general gas constant, λ the Arrhenius pre-exponential factor and T is the absolute temperature.

Results listed in Table 4 showed that the values of E_a determined in 1 M HCl containing ligand L are higher (82.52 $kJ.mol^{-1}$) than that for uninhibited solution (50.73 $Kj.mol^{-1}$) this permit the illustration of Arrhenius plots of log C_R vs .1000/T for the adsorption of compound L in Fig. 3.

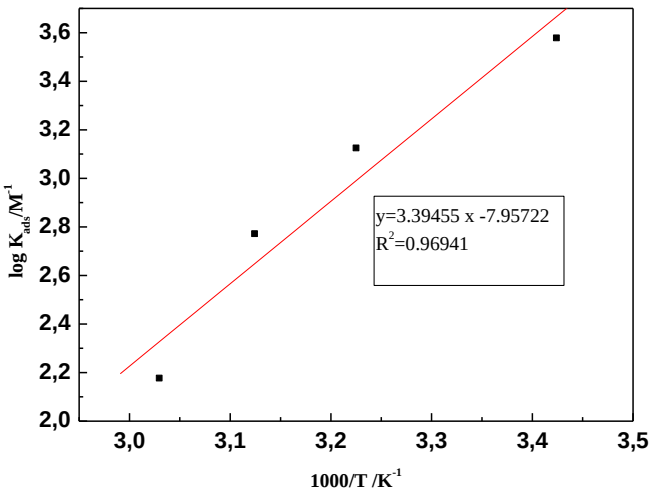

Figure 3. Arrhenius plots of mild steel in 1 M HCl with and without 10^{-3} M of compound L.

The enhancement of apparent activation energy is related to physical adsorption which occurs in the first step as reported by [27, 28], The adsorption decrease is associated to the inhibitor molecules desorption since these two opposite processes are in equilibrium. With higher temperature more desorption of inhibitor occur and lead a great surface of mild steel to a direct contact with aggressive environment. Brandt [29] have also observed likely results concerning corrosion rates increase with enhancement of temperature.

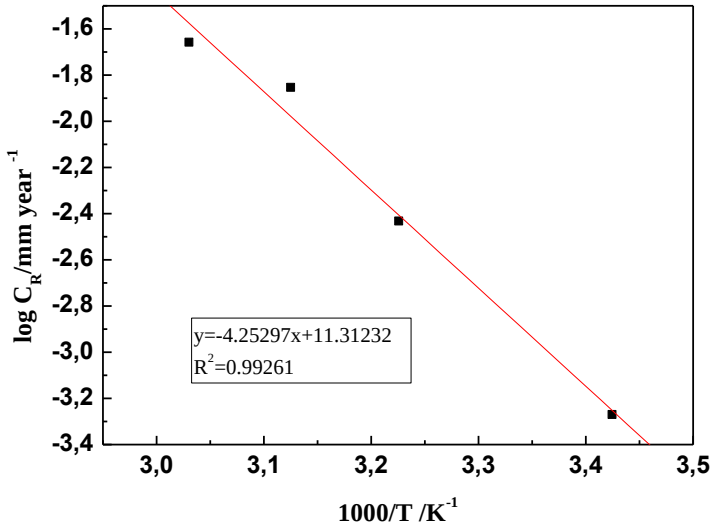

Figure 4. Relation between $\log K_{ads}$ and 1000/T at different temperatures.

Table 4. Evolution with temperature of mild steel parameters in 1M HCl without and with addition of 10^{-3} M compound L.

Temperature (K)	Conc (M)	C_R (mm year^{-1})	η_{WL} (%)	λ (mg cm^{-2}h^{-1})	Ea (kJ mol^{-1})	$\Delta G°_{ads}$ (kJ mol^{-1})	ΔH_{ads} (kJ mol^{-1})	ΔS_{ads} (J mol-1)
292	Blank	0.0026	…	$6.89.10^2$	50.73	…….		……..
	$1·10^{-3}$	0.000537	79	$9.60.10^4$	82.52	-29.72		-120.68
310	Blank	0.0091	…			…….	-64.96	……..
	$1·10^{-3}$	0.0037	57			-28.72		-116.90
320	Blank	0.023	…			…….		……..
	$1·10^{-3}$	0.014	37			-27.63		-116.65
330	Blank	0.025	…			…….		……..
	$1·10^{-3}$	0.022	13			-24.74		-121.87

Inspection of Table 4 showed that $\Delta G°_{ads}$ values decreased with temperature increasing. This fact confirms that inhibitor adsorption is more activated with temperature increase.

With the aid of equation 6 we have been able to draw the plot of ln K_{ads} vs. 1000/T (Fig. 4) which permits to obtain standard enthalpy.

$$\ln K = -\frac{\Delta H°ads}{RT} + \text{constant} \qquad (6)$$

The obtained curve gives straight line with slope equal $\Delta H°_{ads}$ /R. The $\Delta H°_{ads}$ values are also inserted in table 4 and the negative sign of $\Delta H°_{ads}$ values confirmed that the adsorption of inhibitor L was an exothermic process [30].

In an exothermic process, distinction between chemisorption and physisorption could be done by considering the absolute value of $\Delta H°_{ads}$. The chemisorption process $\Delta H°_{ads}$ value approaches 100 Kj. mol^{-1}, while the value is less than 40 $Kj.mol^{-1}$ for the physisorption process [31].

In the present study $\Delta H°_{ads}$ value is about -71 $Kj.mol^{-1}$ indicating that chemical adsorption is preponderant here. Standard entropy of adsorption ($\Delta S°_{ads}$) is then calculated using the basic thermodynamic equation (7):

$$\Delta S^{\circ}_{ads} = \frac{\Delta H^{\circ}_{ads} - \Delta G^{\circ}_{ads}}{T} \quad (7)$$

$\Delta S°_{ads}$ values listed in Table 4, are nearly constant and negative, ranging between -116 and -121 $J.K^{-1}$. mol^{-1} at a temperature range of 292 - 330 K. This is expected since adsorption is an exothermic process and is always accompanied by a decrease of entropy.

3.2. Potentiodynamic polarization

Potentiodynamic polarization curves for mild steel XC48 in 1 M HCl with addition of various concentrations of inhibitor L is depicted in Fig. 5.

Electrochemical corrosion kinetic parameters, such as corrosion potential (E_{cor}), cathodic and anodic Tafel slopes (b_a, b_c), corrosion current density (i_{corr}) which were obtained by Tafel extrapolation method are given in Table 5. Percentage of inhibition efficiency (η_p %) is also given in the same table. η_p was calculated from the polarization measurements according to the equation (8) given below:

$$\eta_p\ \% = \frac{i^{\circ}_{corr} - i_{corr}}{i^{\circ}_{corr}} \quad (8)$$

As illustrated in Fig. 5, the obtained i_{corr} values decrease appreciably with the increase in ligand L concentration up to 10^{-3} M. This may be due to the increase in adsorption of Schiff base on the electrode surface leading to a recovery of a great amount of the surface blocking then the active sites and reducing the metal dissolution [32].

Table 5. Electrochemical parameters for mild steel corrosion in 1M HCl in absence and presence of various concentrations of compound L.

Inhibitor concentration (M)	**E_{corr} (mV/SCE)**	**i_{corr} ($mA.cm^{-2}$)**	***b_a*** **(mV/dec)**	***b_c*** **(mV/dec)**	**η_p (%)**
Blank	-445.1	1.25	439.0	-88.30	……
$1\cdot10^{-5}$	-475.6	0.93	330.3	-113.1	25.6
$5\cdot10^{-5}$	-465.3	0.80	361.4	-104.0	36.0
$1\cdot10^{-4}$	-455.8	0.67	380.5	-73.80	46.4
$5\cdot10^{-4}$	-446.9	0.44	210.0	-50.20	64.8
$1\cdot10^{-3}$	-512.0	0.21	96.80	-26.60	83.2

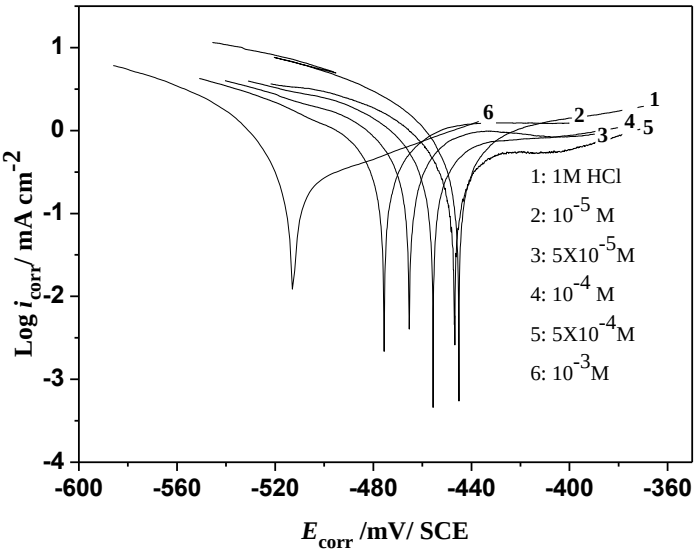

Figure 5. Typical polarization curves for the corrosion of mild steel in 1 M HCl containing different concentrations of compound L at 298 K.

In the presence of compound L the corrosion potential was observed to shift to negative values and the cathodic branches shifted to more negative potential values, the anodic branches exhibit the same change as cathodic branches. It is clear that both cathodic and anodic reactions on XC48 mild steel have been inhibited in the presence of the studied compound. If the displacement in E_{corr} with the addition of inhibitor is less than 85 mV with respect to the corrosion potential of the blank, the inhibitor may be considered as mixed type [33, 34]. Such results reveal that ligand L mainly acts as a mixed type inhibitor. It can also be seen that the addition of this inhibitor retards the hydrogen evolution reaction, which is a cathodic reaction, as observed by Tortato [35].

Table 6. Efficiency comparison in this study with previous works of similar type of compounds.

	Efficiency at optimal concentration in acidic medium *η (%)*			
	Present inhibitor	Hosten [1]	Sulochana [2]	Banerjee [3]
Structure	1-[(3-hydroxy phenyl amino) methylene]-naphtalen-2-one (L)	4-((naphthalen-2-ylimino) methyl)phenol (L1)	N-(2-mercapto phenyl)naphthylide neimine (L2)	2-(2-hydroxy benzylideneamino) phenol (L3)
η (%) In HCl	83.2	91.0	89.8	45.0

On comparing the inhibition efficiency of our compound L with three others L1, L2 and L3 from the literature in Table 6 it is clearly shown that the compounds L, L1, L2 have more beneficial effects on the mild steel surface in a 1M hydrochloric acid solution than the L3 ligand. This means that

the Schiff base derived from the Hydroxynaphthalaldehyde (L, L1, L2) has a better protective capacity than the Schiff base derived from phenol (L3). These compounds are very good Inhibitors and act as mixed inhibitors by reducing the rate of cathodic and anodic reaction. This protection results from the spontaneous adsorption of inhibitor on mild steel surface. The inhibition mechanism obeys Langmuir isotherm. The inhibition efficiency ηp (%) of the L, L1, L2 Schiff base inhibitors is greater than the L3 Schiff base inhibitor [36, 37 ,38].

The temperature effect on inhibition of metal/acid oxidation process was also studied and seemed very complex, as metal surface modifications occur with desorption of inhibitor. The latter may undergo decomposition [39, 40].

Mention that the modification of inhibiting efficiency with the temperature was studied in 1 M hydrochloric acid in presence of the optimum concentration 10^{-3} M of synthesized inhibitor L. It is clearly seen that inhibition efficiency changes considerably with temperature increase {(η_p % = 83,2 (T = 292K), η_p % = 23,15 (T = 328K))}.

3.3. Electrochemical impedance spectroscopy (EIS)

The use of EIS as complementary technique is very helpful as it gives useful information on the electrical behavior of our material in absence or in presence of the synthesized inhibitor L.

The spectroscopic results are given in Fig. 6 (a, b, c). The effects of the compound L concentration on the electrochemical impedance spectroscopy behavior of mild steel XC48 in 1 M HCl solution were investigated at the open circuit potential condition.

The Nyquist plots of mild steel XC48 in the absence and in the presence of various concentrations of the inhibitor L are shown in Fig. 6 a and the related Bode plots with phase –angle curves are represented in Fig. 6 (b, c).

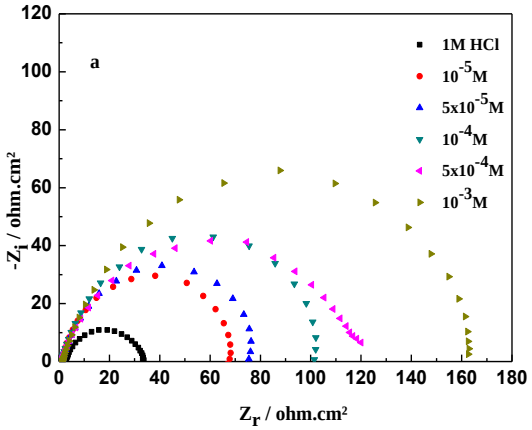

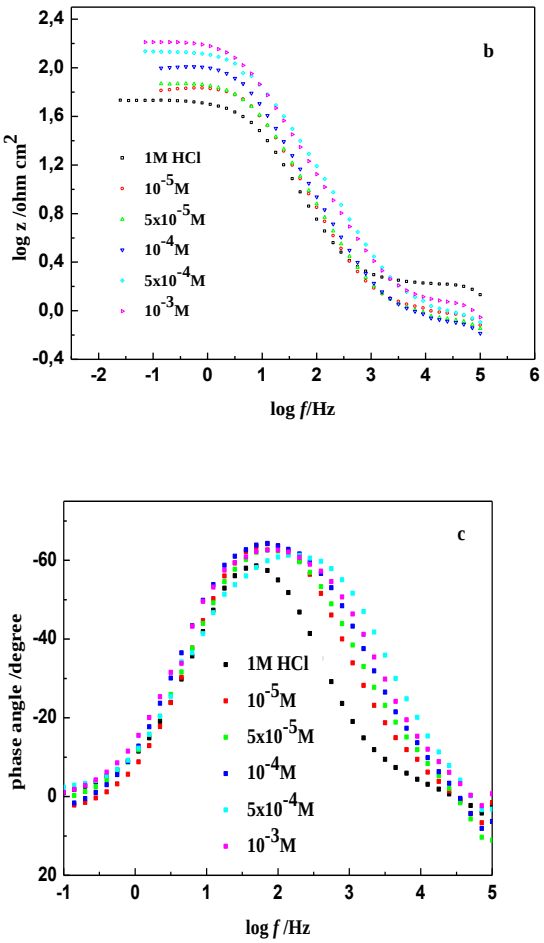

Figure 6. Impedance diagrams for the mild steel in 1 M HCl at 298 K containing various concentrations of compound L, (a) Nyquist plots (b) Bode plots and (c) phase angle plots obtained at room temperature.

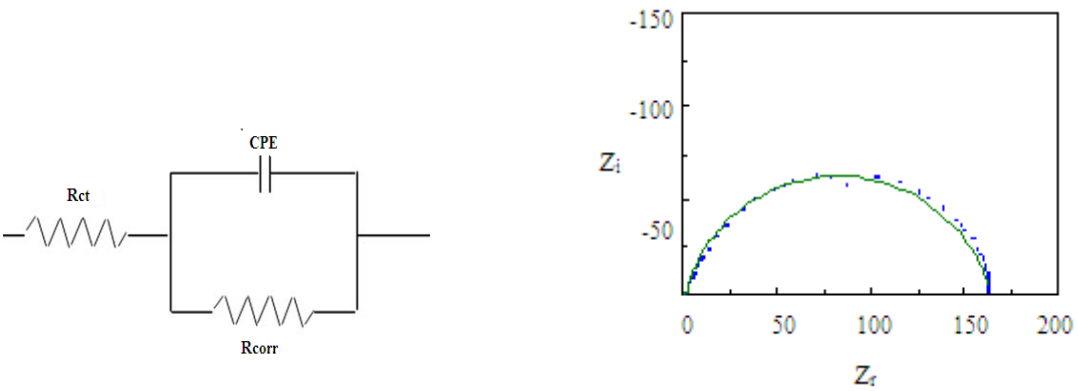

Figure 7. Nyquist plot of mild steel XC48 and its fitting in 1 M HCl in presence of inhibitor L at concentration of 10^{-3} M.

Generally, all the Nyquist plots show not perfect semi-circles which indicate activation – controlled reactions with single charge transfer. Nyquist plot is modeled by a simple electric circuit

including the charge transfer resistance (R_{corr}) parallel with a constant phase element CPE in series with solution resistance (R_s) is illustrated in Fig. 7 with the fitting curve. It has to be mentioned that the experimental data were in good agreement with the experimental model reported in the literature. The Nyquist plots of both experimental and simulated data presented in Fig. 7 give a reasonable accuracy of fit in the order of 10^{-3} M.

The use of CPE can explain the difference between the experimental behavior and the theory by non-ideal behavior of double layer as a capacitor instead of double layer capacity. This CPE can be modeled as follows according to the equation (9) [41]:

$$Z_{CPE} = (j\omega C)^{-\alpha} \quad (9)$$

Where Z_{CPE} is the impedance, j is the square root of -1, ω the frequency, C the capacitance, and α is a measure of the capacitor of non-ideality of double layer and has a value in the range of $0 < \alpha < 1$.

Table 7 shows the impedance parameters deduced from Nyquist plots of the Schiff base in different concentrations. Inhibition efficiency η_z % was calculated through the following equation (10):

$$\eta_z\,\% = \frac{R_{ct}^{-1} - R_{ct(inh)}^{-1}}{R_{ct}^{-1}} \quad (10)$$

According to this table, the charge transfer resistance of mild steel increased highly in the presence of the inhibitor L, causing the decrease of the metal corrosion. This increase may be due to the important adsorption of inhibitor molecules on the metal surface at higher concentrations, leading to a greater surface coverage.

The CPE values were found to decrease with the increasing inhibitor L concentration. This behavior is usually obtained for systems where inhibition takes place after formation of a surface film by adsorption of the inhibitor L on the metal surface [42, 43, 44]. The CPE decrease was probably caused by the thickness increase of the electrical double layer. Such a behavior suggests that the inhibitor molecules act by adsorption at the metal/solution interface as confirmed before by[45, 46].

Table 7. Impedance parameters for corrosion of mild steel XC48 in 1M HCl in the absence and presence of different concentrations of compound L.

Inhibitor concentration (M)	Rs (Ωcm^2)	Rct (Ωcm^2)	CPE ($\Omega^{-1}cm^{-2}Sn$)	A	C_{dl} (μFcm^{-2})	η_Z (%)
Blank	2.38	31.58	$43.96.10^{-4}$	0.75	2276	
$1{\cdot}10^{-5}$	0.99	69.00	$45.61.10^{-5}$	0.88	284	54.23
$5{\cdot}10^{-5}$	1.20	78.00	$38.99.10^{-5}$	0.89	253	59.51
$1{\cdot}10^{-4}$	0.85	104.0	$36.18.10^{-5}$	0.88	235	69.63
$5{\cdot}10^{-4}$	0.94	138.0	$35.18.10^{-5}$	0.80	165	77.11
$1{\cdot}10^{-3}$	1.15	163.0	$31.95.10^{-5}$	0.84	181	80.74

It has to be noticed that α values are between (0.80 and 0.89) suggesting the presence of capacitive behavior and the C_{dl} calculated values decrease by the same manner than CPE, however the change in C_{dl} observed for 10^{-3} M, may be explained by the gradual displacement of water molecules

caused by the adsorption of the organic molecules on mild steel, causing the diminution of the metal dissolution amount [47].

The results obtained by electrochemical measurements are seen to be in agreement to each other.

3.4. Effect of immersion time and corrosion attack morphology

Immersion time experiments in the present work were carried out by immersing initially the metal in 1 M hydrochloric acid containing 10^{-3} M of compound L at 24, 48 h and 96 h.

The morphological aspect of the mild steel surfaces in absence and presence of our inhibitor L after 24, 48 and 96 hrs have been investigated using optical microscopy . The related images are presented in Fig. 8 (a, b, c, d) respectively.

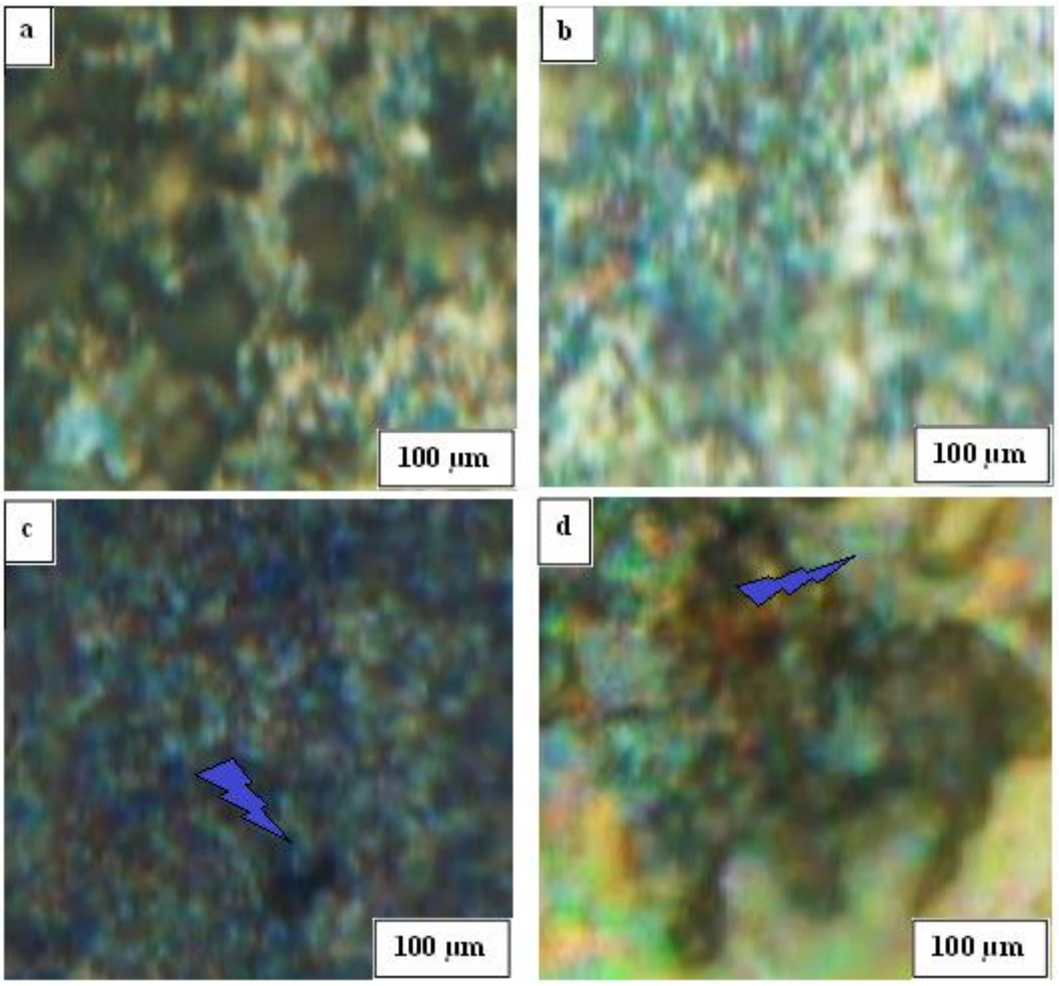

Figure 8. Surface mild steel morphology after immersion time of 24 h (a) in 1 M HCl solution, (b) in the presence of 10^{-3} M in situ synthesized inhibitor L, (c) after 48 h and (d) 96 h.

The micrographs show a strongly damaged surface with important pits for the specimen immersed in 1 M HCl solution for 24 hrs without inhibitor. In the presence of the inhibitor L, the

corrosion attack seems to decrease for the period of 24 h and continues till 48 h. However, with long immersion periods, the surface exhibits a large attacked zone. Such a behavior could be explained by the formation of hemimicelle aggregates by the initially deposited inhibitor molecules, which reduce the effective area covered by the inhibitor L and the non covered sites are subject to the chloride attack as reported by Bastos [48]. However after a long period the surface is subject to the chloride attack again may be due to the inhibitor L desorption from the surface leading a non covered surface.

3.5. Adsorption phenomenon and mechanism

Interaction between the inhibitor molecules and the mild steel surface can occur in terms of the adsorption isotherm.

The linear dependence of C_{inh}/Θ versus (C_{inh}), drawn from experimental parameters of weight loss data, Tafel slopes and EIS (Fig. (2, 9)) permits the adsorption constant values to be calculated. The correlation R^2 for all methods was very close to 1, indicating that the adsorption process of L on metal surface obeyed the Langmuir isotherm. It is worth nothing that the values of standard Gibbs free energy determined by the three methods are similar; we found -33 kJ mol1 by weight loss data, -32.49 kJ mol1 by Tafel slopes and -33.28 kJ mol1 by EIS measurements.

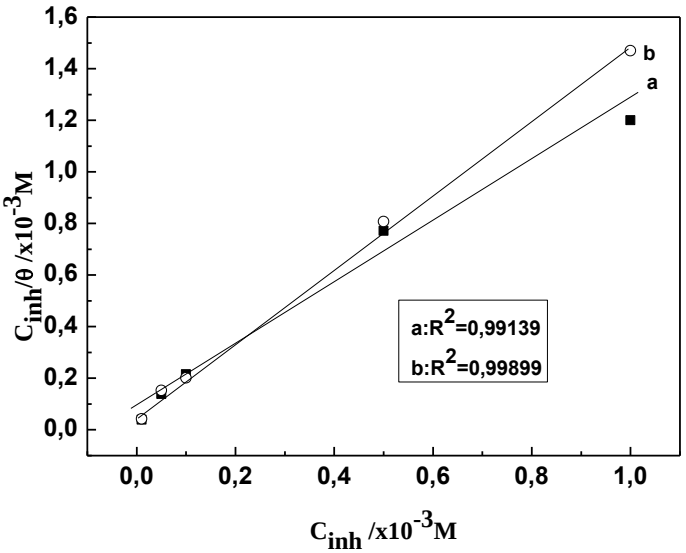

Figure 9. Langmuir adsorption isotherm plot Potentiodynamic polarization (a) and impedance (b) for the adsorption of compound L at mild steel/ hydrochloric acid interface.

According to the literature, immersion in hydrochloric acid solution suggests the following mechanism for the corrosion of iron and steel [49, 50]. For anodic dissolution the proposed mechanism is as follows:

$$Fe + Cl^- \leftrightarrow (FeCl^-)_{ads} \quad (a)$$

$$(FeCl^-)_{ads} \leftrightarrow (FeCl)_{ads} + e^- \quad (b)$$

$$(FeCl)_{ads} \rightarrow (FeCl^+) + e^- \quad (c)$$

$$(FeCl^+) \leftrightarrow Fe^{++} + Cl^- \quad (d)$$

After immediate immersion of mild steel in HCl solution including the inhibitor, chloride ions are firstly adsorbed onto the ionized metal surface by coulomb attraction. Inhibitor molecules could be adsorbed through electrostatic interactions with the iron chloride. The previous iron–chloride form products between the positively charged molecules and the negatively charged metal surface [51].

In fact, inhibitor molecules interact with $(FeCl^-)_{ads}$ species giving monomolecular layers on the steel surface. These complex films prevented mild steel surface from direct attack by chloride ions. Thus, the oxidation reaction of $(FeCl^-)_{ads}$ can be prevented.

Thereby at cathodic sites the adsorption of protonated Schiff base molecules occur in competition with hydrogen ions that are going to reduce according to $2H^+ + 2e^- \rightarrow H_2$ by the following mechanism:

$$Fe + H^+ \leftrightarrow (FeH^+)_{ads} \quad (e)$$

$$(FeH^+)_{ads} + e^- \rightarrow (FeH)_{ads} \quad (f)$$

$$(FeH)_{ads} + H^+ + e^- \rightarrow Fe + H_2 \quad (g)$$

3.6. Theoretical Calculation

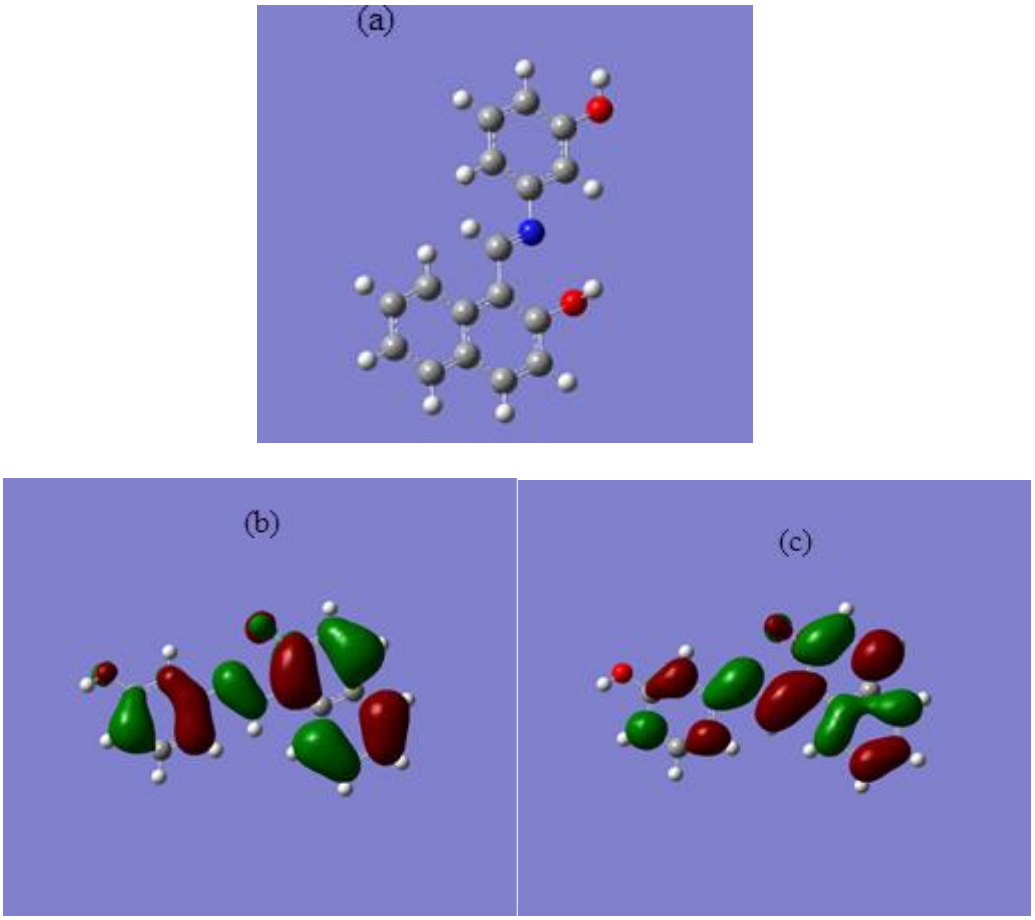

Figure 10. Frontier molecule orbital density distributions of the synthesized inhibitor.

Quantum chemical calculation has potential application in designing and subsequent development of several organic corrosion inhibitors in the field of corrosion inhibition chemistry.

Density functional theory (DFT) based computational methods is very useful technique in studying the correlation between the molecular structure of the inhibitors and its corrosion inhibition capability [52].

Relevant quantum chemical parameters of the studied Schiff base L including the HOMO energy (E_{HOMO}), the LUMO energy (E_{LUMO}), the energy gap ($\Delta E = E_{LUMO} - E_{HOMO}$), the global hardness ($\eta$), the absolute electronegativity (χ), the fraction of the transferred electrons (ΔN) and dipole moment (μ) are listed in Table 7. The optimized structures of the compound L studied are given in Fig.10.

The reactive abilities of hydroxyl derivative are closely related to their frontier molecular orbitals including the highest occupied molecular orbital (HOMO) and the lowest unoccupied molecular orbital (LUMO). E_{HOMO} indicates the tendency of an organic molecule to donate electrons. The higher the value of E_{HOMO}, the greater the ability of a molecule to donate electrons while E_{LUMO} indicates the propensity of a molecule to accept electrons. Thus, the binding ability of organics to the metal surface increases with an increase in energy of the HOMO and a decrease in the value of energy of the LUMO. The energy gap, ΔE, is an important parameter which indicates the reactivity tendency of organics toward the metal surface [53]. These results show that ligand L is a good corrosion inhibitor for mild steel in 1 M HCl

Mention that The most widely used quantity to describe the polarity is the dipole moment of the molecule [54]

The high value of dipole moment probably increases the adsorption between chemical compound and metal surface [55]. In our study, the value of the dipole moment of ligand L is 3.2932 Debye is more than that of μ_{H2O} (1.88 D).

ΔN shows inhibition efficiency resulting from electrons transferred from the inhibitor molecule to the iron atom [56]. According to Zucchi [57], if the value of ΔN is less than 3.6 the efficiency of inhibition increases with increasing electron-donating ability of the inhibitor at the metal surface. In this study, the value of $\Delta N = 0.8627 < 3.6$ (Table 8) therefore the molecules of the inhibitor are electron donors to the metal surface which is an acceptor.

The data obtained from quantum chemical calculations give good evidence on the obtained results by weight loss and electrochemical techniques.

Table 8. Calculated quantum chemical parameters of compound L

Quantum parameters	compound L
E_{HOMO} (eV)	-5.6063
E_{LUMO} (eV)	-1.7646
$\Delta E_{LUMO-HOMO}$ (eV)	3.8416
dipole moment (μ)	3.2932
$I = -E_{HOMO}$	5.6063
$A = -E_{LUMO}$	1.7646
$\chi = \frac{I+A}{2}$ (eV)	3.6855
$\eta = \frac{I-A}{2}$ (eV)	1.9208
$\sigma = \frac{1}{\eta}$ (eV)	0.5206
ΔN	0.8627

4. CONCLUSION

The new Schiff base 1-[(3-hydroxyphenylamino) methylene]-naphtalen2-one (L) was synthesized and confirmed by using X-ray crystallographic technique.

Experimental data show that 1-[(3-hydroxyphenylamino) methylene]-naphtalen2-one (L) inhibitor is an effective inhibitor for the corrosion of mild steel XC48 in a 1M HCl. Inhibition efficiency increases with the studied inhibitor concentration enhancement, but decreases with the increase in temperature, it further leads to an increase in activation energy.

The less negative $\Delta G°_{ads}$ values suggest the spontaneous adsorption and the $\Delta H°_{ads}$ values determined the preponderant chemisorption process of the inhibitor on the metal surface.
Potentiodynamic polarization curves indicated that the ligand L acted as mixed type in HCl solution.

The adsorption of ligand Schiff bases L on mild steel surface obeyed the Langmuir adsorption isotherm.

The electrochemical impedance study (EIS) measurements showed an increase of Rct value with the addition of the inhibitor L, while the CPE value decreased, indicating the formation of a protected film at the surface.

The optical morphological investigation shows the decrease of the pits resulting from chloride attack with the presence of the inhibitor L.

For further confirmation of the result, the values of inhibition efficiency obtained from weight loss, polarization study and EIS measurements were correlated with theoretical values obtained through DFT calculations.

ACKNOWLEDGEMENTS
The authors are indebted to the University of Setif-1 (UFAS), whose responsible provided financial support for the conduct of this research.

References

1. G. Trabanelli, *Corrosion*, 47 (1991) 410.
2. K.C. Emregül, R. Kurtaran and O. Atakol, *Corrosion Science*, 45 (2003) 2803.
3. F. Bentiss, C. Jama, B. Mernari, H. El Attari, L. El Kadi, M. Lebrini, M. Traisnel and M. Lagrenee, *Corrosion Science*, 51 (2009) 1628.
4. C. Kustu, KC. Emregül and O. Atakol, *Corrosion Science*, 49 (2007) 2800.
5. K.C. Emregül, E. Duzgun and O. Atakol, *Corrosion Science*, 48 (2006) 3243.
6. H. Ashassi-Sorkhabi, B. Shaabani and D. Seifzadeha, *Electrochimica Acta*, 50 (2005) 3446.
7. M. Lebrini, M. Lagrenee, H. Vezin, M. Traisnel and F. Bentiss, *Corrosion Science*, 49 (2007) 2254.
8. H.D. Lece, K.C. Emregül and O. Atakol, *Corrosion Science*, 50 (2008) 1460.
9. A. Barbosa da Silva , E. D'Elia and J.A. da Cunha Ponciano Gomes, *Corrosion Science*, 52 (2010) 788.
10. I.B. Obot, N.O. Obi-Egbedi and S.A. Umoren, *Corrosion Science*, 51 (2009) 1868.
11. N.A. Negm and M.F. Zaki, *Colloids and Surfaces A*, 322 (2008) 97.
12. E.A. Noor, *Materials Chemistry and Physics*, 114 (2009) 533.

13. Z. Da-Quan, C. Qi-Rui, H. Xian-Ming, G. Li-Xin and Z. Guo-Ding, *Materials Chemistry and Physics*, 112 (2008) 353.
14. M. Hosseini, S.F.L. Mertens, M. Ghorbani and M.R. Arshadi, *Materials Chemistry and Physics*, 78 (2003) 800.
15. F. Bentiss, M.Traisnel and M. Lagrenee, *Journal of Applied Electrochemistry*, 31 (2001) 41.
16. S. Muralidharan, R. Chandrasekar and S.V.K. Iyer, *Proceedings of the Indian Academy Of Science*, 112 (2000) 127.
17. Z. Popovic, G. Pavlovic, D. Matkovic, C. alogovic, V. Roje and I. Leban, *Journal of Molecular Structure*, 615 (2002) 23.
18. H. Ünver, M. Yıldız, A. Kiraz and Ö. Özgen, *Journal of Chemical Crystallography*, 39 (2009) 17.
19. S. Chahmana, F. Benghanem, S. Keraghel and A. Ourari, *Acta Crystallographica Section E*, 70 (2014) 107.
20. B. Kaitner and G. Pavlovic, *Acta Crystallographica Section C*, 52 (1996) 2573.
21. A. Özek, S. Yüce, C. Albayrak, M. Odabasoglu and O. Büyükgüngör, *Acta Crystallographica Section E*, *6*0 (2004) 356.
22. A.K. Singh, M.A. Quraishi, *Corrosion Science*, 52 (4) (2010) 1529.
23. T.D. Burleigh, *Corrosion*, 45 (6) (1989) 464.
24. P. Morales-Gil, G. Negrón-Silva, M. Romero-Romo, C. Ángeles-Chávez and M. Palomar-Pardavé, *Electrochimica Acta*, 49 (2004) 4733.
25. F. Mansfeld, Corrosion Mechanisms, Marcel Dekker, NewYork, 1987, p. 119.
26. E.A. Noor and A.H. Al-Moubaraki, *Materials Chemistry and Physics*, 110 (2008) 145.
27. S. Martinez and I. Stern, *Applied Surface Science*, 199 (2002) 83.
28. A. Ghazoui, N. Benchat, F. El-Hajjaji, M. Taleb, Z. Rais, R. Saddik, A. Elaatiaoui and B. Hammouti, *Journal of Alloys and Compounds*, 693 (2017) 510.
29. T. Szauer and A. Brandt, *Electrochimica Acta*, 26 (1981) 1257.
30. M.A. Badawi, M.A. Hegazy, A.A. El-Sawy, H.M. Ahmed and W.M. Kamel, *Materials Chemistry and Physics*, 124 (2010) 458.
31. M.A. Hegazy, A.M. Hasan , M.M. Emara, M.F. Bakr and A.H. Youssef, *Corrosion Science*, 65(2012)67.
32. H. M. Abd El-Lateef and A. H. Tantawy, *RSC Advances*, 6 (2016) 8681.
33. M. Behpour, *Journal of Materials Science*, 44 (2009) 2444.
34. E.P. Manuel, O-X. Crescencio o, V.L Natalya and P-N. Jonathan-Boanerge, *Journal of Surfactants and Detergent*s, 14 (2011) 211
35. G. Quartarone, L. Bonaldo and C. Tortato , *Applied Surface Science*, 252 (2006) 8251.
36. E.E. Elemike, H.U. Nwankwo, D.C. Onwudiwe and E.C. Hosten, *Journal of Molecular Structure*, 1147 (2017) 252.
37. D. Kesavan, M. Gopiraman, R. Karvembu, M.M. Tamizh and N. Sulochana, *Journal of Surfactants and Detergent*, 15 (2012) 567.
38. S.Kr. Saha, A. Dutta, P. Ghosh, D. Sukul and P. Banerjee, *Physical Chemistry Chemical Physics*, 17 (2015) 5679.
39. J. Alijourani, K. Raeissi and M.A. Golozar , *Corrosion Science*, 51 (2009) 1836.
40. S. Girija, U.K. Mudali, V.R. Raju, R.K. Dayal, H.S. Khatak and B. Raj, *Materials Science and Engineering A*, 407 (2005) 188.
41. D.F. Roeper, D. Chidambaram, C.R. Clayton and G.P. Halada, *Electrochimica Acta*, 53 (2008) 2130.
42. K.C. Emregül and O. Atakol, *Materials Chemistry and Physics*, 83 (2004) 373.
43. I.L. Rosenfield, Corrosion Inhibitors, McGraw-Hil, New York, 1981, p.301.
44. H.M. Abd El-Lateef, *Corrosion Science*, 92 (2015) 104.
45. F. Bentiss, M. Traisenl and M. Lagrenee, *Corrosion Science*, 42 (2000) 127.

46. S. Murlidharan, K.L.N. Phani, S. Pitchumani, S. Ravichandran and S.V.K. Iyer, *Journal of The Electrochemical Society*, 142 (1995) 1478.
47. M. Benabdellah, R. Touzani, A. Aounitia , A. Dafali , S. El Kadiri, B. Hammouti and M. Benkaddour , *Materials Chemistry and Physics*, 105 (2007) 373.
48. Z. Ait Chikh, D. Chebabe, A. Dermaj, N. Hajjaji, A. Srhiri, M.F. Montemor, M.G.S. Ferreira and A.C. Bastos, *Corrosion Science*, 47 (2005) 447.
49. A. Yurt, A. Balaban, S.U. Kandemir, G. Bereket and B. Erk, *Materials Chemistry and Physics*, 85 (2004) 420.
50. A. Rubaye, A. Abdulwahid, S. Al-Baghdadi, A. Al-Amiery, A. Kadhum and A. Mohamad, *International Journal of Electrochemical Science*, 10 (2015) 8200.
51. M.A. Quraishi, M.Z.A. Rafiquee, S. Khan and N. Saxena, *Journal of Applied Electrochemistry*, 37 (2007) 1153.
52. M.J. Bahram, S.M.A. Hosseini and P. Pilvar, *Corrosion Science*, 52 (2010) 2793.
53. A. Aytac, S. Bilgic, G. Gece, N. Ancin and S.G. Oztas, *Materials and Corrosion*, 63 (8) (2012) 729.
54. E.E. Ebenso, D.A. Isabirye and N.O. Eddy, *International Journal of Molecular Sciences*, 11 (2010) 2473.
55. I. Ahamad, S. Khan, K.R. Ansari and M.A. Quraishi, *Journal of Chemical and Pharmaceutical Research*, 3 (2011) 703.
56. K.F. Khaled, *Corrosion Science*, 52 (2010**)** 3225.
57. I. Lukovits, E. Kálmán and F. Zucchi, *Corrosion*, 57 (1) (2001) 3.